

# Measuring the muon content of inclined air showers using AERA and the water-Cherenkov detector array of the Pierre Auger Observatory

---

**Marvin Gottowik<sup>a,\*</sup> for the Pierre Auger Collaboration<sup>b</sup>**

<sup>a</sup>*Instituto Galego de Física de Altas Enerxías (IGFAE), Universidade de Santiago de Compostela, Santiago de Compostela, Spain*

<sup>b</sup>*Observatorio Pierre Auger, Av. San Martín Norte 304, 5613 Malargüe, Argentina*

*Full author list:* [https://www.auger.org/archive/authors\\_icrc\\_2023.html](https://www.auger.org/archive/authors_icrc_2023.html)

*E-mail:* [spokespersons@auger.org](mailto:spokespersons@auger.org)

In this proceeding, we present a proof of principle study for estimating the number of muons of inclined air showers proportional to their energy using hybrid radio and particle detection. We use the radiation energy of an air shower to estimate its electromagnetic energy and measure the muon number independently with the water-Cherenkov detector array (WCD) of the Pierre Auger Observatory. We select 32 high-quality events in almost six years of data with electromagnetic energies above 4 EeV to ensure full efficiency for the WCD reconstruction. The muon content in data is found to be compatible with the one for an iron primary as predicted by current-generation hadronic interaction models. This can be interpreted as a deficit of muons in simulations as a lighter mass composition is expected from  $X_{\max}$  measurements. Such a muon deficit was already observed in previous analyses of the Auger collaboration and is now confirmed for the first time with radio data. Currently, this analysis is limited by low statistics due to the small area of AERA of  $17 \text{ km}^2$  and the high energy threshold. We will outline the advantages of using radio detection instead of the Auger Fluorescence Detector in future analyses allowing for high-statistic measurements of the muon content as a function of energy.

38th International Cosmic Ray Conference (ICRC2023)  
26 July - 3 August, 2023  
Nagoya, Japan



---

\*Speaker

## 1. Introduction

Ultra-high energy cosmic rays can only be observed indirectly through air showers initiated in the Earth's atmosphere. The mass composition of cosmic rays can be inferred from certain shower observables such as the depth of the shower maximum,  $X_{\max}$ , and the number of muons. The muon number at ground-level increases nearly linearly with the cosmic-ray energy and with the mass of the cosmic ray. The interpretation of the measured muon number in data relies on the comparison with predictions made by full Monte-Carlo air-shower simulations based on hadronic interaction models. Previous studies performed by the Pierre Auger collaboration, but also at other experiments have shown a deficit of muons predicted by all current-generation hadronic interaction models compared to data [1].

The potential of a combined analysis of the radio emission and the muons was already shown for simulations [2]. In this proceeding, a new method to measure the muon content of inclined air showers with zenith angles above  $60^\circ$  using hybrid radio and particle detections at the Pierre Auger Observatory is presented. The feasibility of detecting and reconstructing such air showers with AERA has been demonstrated [3, 4]. For inclined air showers, the water-Cherenkov detector (WCD) performs an almost pure measurement of the muons, other particles are mostly absorbed in the atmosphere and do not reach the ground. However, the radio emission of the air shower can still be detected on the ground as there is neither significant absorption nor scattering in the atmosphere. The radio emission originates from the electromagnetic component of the air shower and allows the reconstruction of its energy. Hence, the electromagnetic energy and the muon content can be reconstructed independently.

## 2. AERA and the water-Cherenkov detector array of the Pierre Auger Observatory

The Pierre Auger Observatory is a multi-hybrid detector for the measurement of ultra-high-energy cosmic rays located in Mendoza, Argentina [5]. Its baseline detectors comprise the world's largest Surface Detector (SD) and a Fluorescence Detector (FD) overlooking the array from 4 sites with 27 telescopes. The SD consists of 1600 water Cherenkov particle detectors deployed on a hexagonal grid with a spacing of 1500 m covering an area of 3000 km<sup>2</sup>. For inclined air showers, it is fully efficient for primary energies above 4 EeV. The Auger Engineering Radio Array (AERA) [6] is located in the northwestern part of the SD. AERA consists of 153 radio stations distributed over an area of 17 km<sup>2</sup>. It was deployed in 3 phases and contains two different kinds of electronics, a self-triggered part and one that is triggered externally. The layout of AERA is shown in Fig. 1. Only radio stations that can provide data on an external trigger are used in this analysis. This amounts to 76 stations before 2 March 2015 (AERA phase II). Afterwards, 29 additional radio stations have been deployed (AERA phase III).

The high energy threshold of the SD combined with the rather small area of AERA makes it challenging to gather high statistics. Therefore, we will not be able to provide a high precision measurement of the muon number in air showers. However, this work is meant as a proof of concept showing the feasibility of such a measurement. Using a radio detector instead of the FD has the benefit of an uptime of almost 100 % whereas the FD has an uptime of  $\sim 15 \%$ . Furthermore, the geometrical phase space for high-quality event reconstructed with the FD is small for inclined

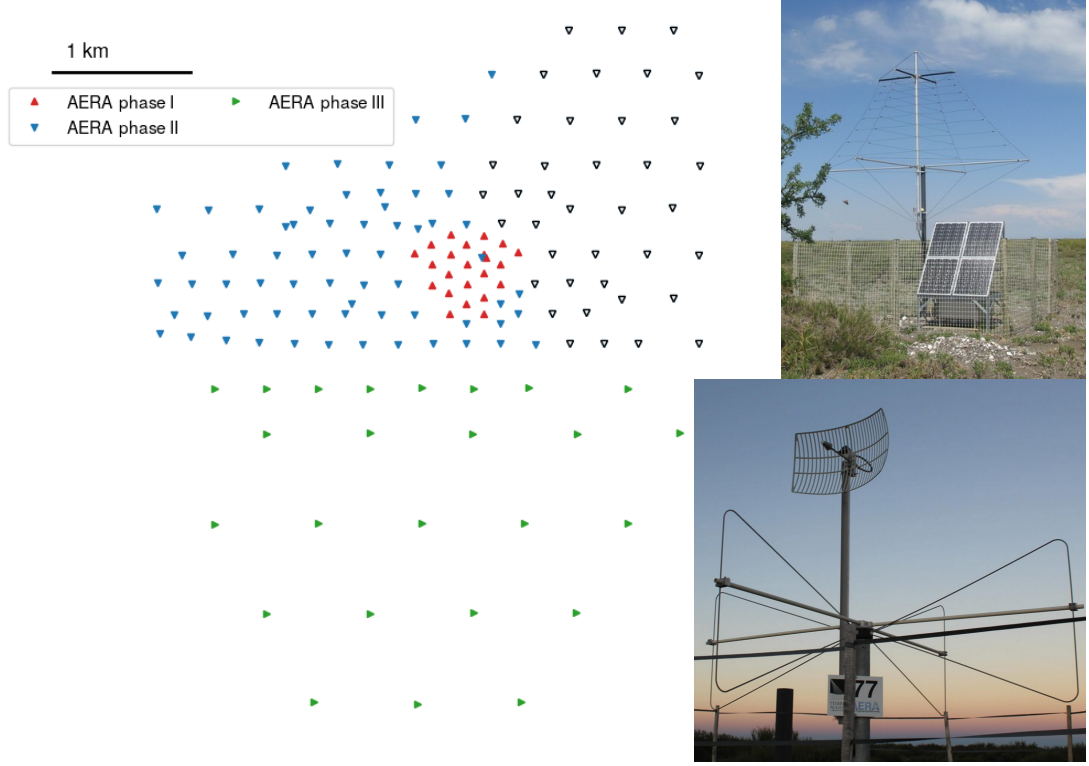


**Figure 1:** Schematic map of AERA (left). The orientation of the triangles indicate the three deployment phases, empty triangles denote stations that are operated in self-trigger mode. Pictures of the two different antenna types used at AERA (right) [7]. Top picture shows an LPDA antenna used for AERA phase I, bottom pictures shows a butterfly antenna used for AERA phase II and III.

showers as a high fraction of air showers have the  $X_{\max}$  outside of the field of view of the telescopes. Such a selection is not needed with a radio detection hence one can collect data more efficiently.

The total muon number is reconstructed by rescaling two-dimensional reference maps of the lateral muon density to the measured signals of the WCD stations. The rescaling factor can be interpreted as a relative muon number,  $R_\mu$ , with respect to the reference model, proton showers simulated at an energy of  $10^{19}$  eV using QGSjetII-03 as hadronic interaction model [8]. An example of such a reference map is shown in Fig. 2 (left) for a zenith angle of  $84^\circ$ .

The lateral distribution of the radio signal is described with a model made for inclined air showers [9]. An example of a fitted lateral distribution function (LDF) for an event with a zenith angle of  $(70.1 \pm 0.1)^\circ$  coming from  $(10.36 \pm 0.03)^\circ$  west of south is shown in Fig. 2 (right). Integrating the LDF over the whole footprint yields the total radiation energy,  $S_{\text{rad}}$ , which is directly related to the energy of the electromagnetic particle cascade  $E_{\text{EM}}$  [10]. A full reconstruction of the primary energy from the radio data also requires an estimate of the contribution of non-electromagnetic energy. This will be done in the future in a data driven method similar to [11], together with a detailed study of the systematic uncertainties. For the present work, data is presented as a function of the total radiation energy  $S_{\text{rad}}$ , while the highest energy events are selected according to the conversion described in [9].

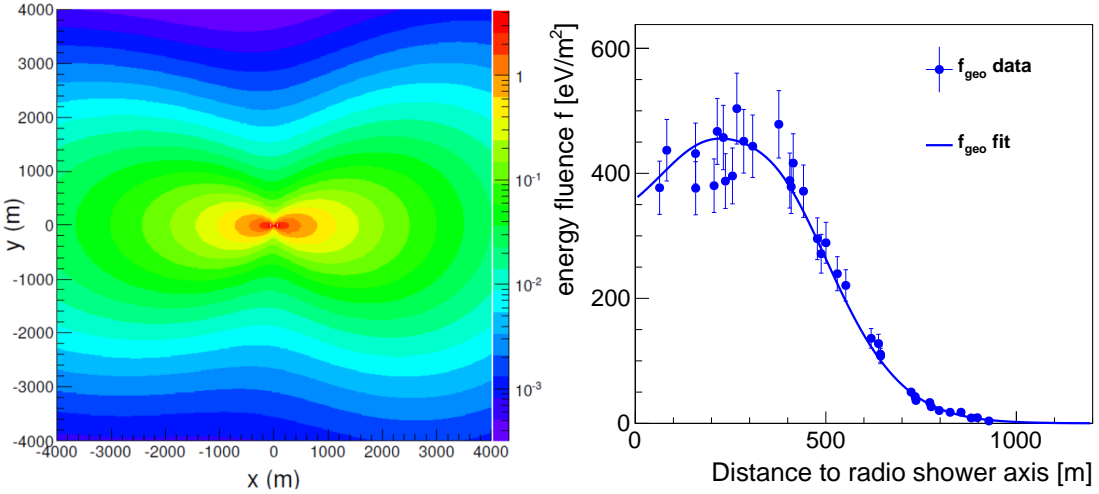


**Figure 2:** Contour plot of the average muon density in the shower plane for a 10 EeV proton showers with a zenith angle of  $84^\circ$  (left). The y-axis is oriented in the direction of the magnetic field projected onto the shower plane. Figure from [8]. Distribution of the radio signal as a function of the distance from the shower axis (right) for an event passing the high-quality event selection, cf. Tab 1. A signal is found for 37 antennas.

### 3. Predicted muon content in simulations

The scaling of the muon content as a function of  $S_{\text{rad}}$  as predicted in simulations is derived by simulating more than 100 000 inclined air showers with CORSIKA [12] using QGSjetII-04 [13], EPOS-LHC [14], and Sibyll 2.3d [15] as hadronic interaction models. The simulations are made using protons and iron nuclei as primaries with energies between  $10^{18.4}$  eV and  $10^{19.6}$  eV. For each simulated air shower the total number of muons is counted and divided by a reference muon number. This reference is obtained from a zenith-angle dependent parametrization of the total muon number based on QGSjetII-03 simulations. The electromagnetic energy of the air shower is given by the sum of the energy deposited by all electromagnetic particles. This is converted to the corresponding  $S_{\text{rad}}$  based on [9]. Fitting a power law results in the dashed and dash-dotted lines in Fig. 3 for each primary and hadronic interaction model.

The performance of the reconstruction is validated with a set of more than 1000 air showers simulated with CoREAS [16] using QGSjetII-04 as hadronic interaction model and proton and iron nuclei as primary particles. The geometry and energy are sampled randomly and cover the full phase space of possible event detection. Showers were generated with energies between 2 EeV and 40 EeV and zenith angles between  $58^\circ$  and  $82^\circ$ . The core positions were randomised such that a sufficient number of antennas is expected to be within a maximum of three Cherenkov radii <sup>1</sup>. The simulations are reconstructed including a realistic detector simulation and the addition of measured environmental noise from randomly selected timestamps.

A high-quality event selection is applied which limits the zenith-angle range from  $60^\circ$  to  $80^\circ$ . Furthermore, signals must be measured in a complete hexagon of SD stations around the station with the largest energy deposit. This yields a bias-free energy reconstruction (estimated from the

<sup>1</sup>The radius of the Cherenkov ring in the shower plane increases from  $\sim 200$  m at a zenith angle of  $60^\circ$  to more than 700 m at  $80^\circ$ .

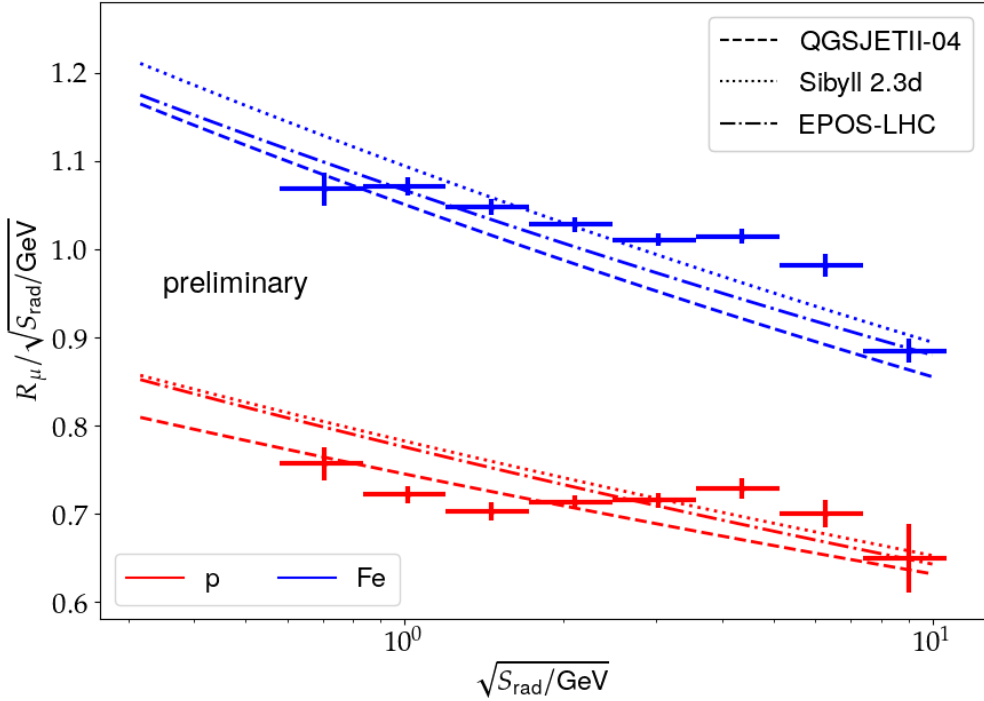


**Figure 3:** The different lines represent the predicted muon content of proton and iron induced air showers for three different hadronic interaction models. The different primary particles are denoted by color, the models by the linestyle. The profile indicates the reconstructed average muon content for discrete energy bins, the y-uncertainty is given by the uncertainty of the mean. See text for details.

number of muons) with a resolution of 19.3 % for events with a primary energy above the full efficiency threshold of 4 EeV [8]. The radio events need to have a successful LDF fit and a signal from a station inside of the Cherenkov ring. To ensure a high quality of the fit result more than 5 signal stations are required and the reduced  $\chi^2$  needs to be smaller than 5. As we only have direct access to the electromagnetic energy, but not the primary energy we require that  $E_{EM}$  is above 4 EeV, which guarantees a primary energy above the full efficiency threshold. Occasionally the reconstruction exhibits large uncertainties. We select events with a relative uncertainty on the reconstructed  $E_{EM}$  below 20 %. Events that have an opening angle between the shower direction reconstructed with the WCD and AERA larger than  $2.08^\circ$  are removed from the analysis. The threshold is given by the mean value plus three standard deviations of a Gumble fit to the full opening angle distribution [17].

The profile of the reconstructed values is shown in Fig. 3. It is fluctuating around the model line for proton primaries but exhibits a bias for iron nuclei. This bias originates from an energy-dependent bias in the  $E_{EM}$  reconstruction as the used LDF model is developed for the AugerPrime Radio Detector [18] and not yet optimized for AERA. It can likely be improved with an optimized LDF in the future. For the sake of the here presented proof-of-concept, study there is a sufficiently good agreement of the reconstruction with the model prediction.

**Table 1:** Number of events after each cut starting with 2663 reconstructed events. The first set of cuts is related to the WCD reconstruction, the second one to the AERA reconstruction.

| cut  | number of events after cut |
|--|----------------------------|
| $60^\circ \leq \theta_{SD} \leq 80^\circ$          | 2002                       |
| number of candidate stations $\geq 5$              | 1108                       |
| Full hexagon of stations                           | 953                        |
| no thunderstorm conditions                         | 849                        |
| SD-RD opening angle $< 2.08^\circ$                 | 788                        |
| has LDF fit with a station inside Cherenkov radius | 532                        |
| $E_{EM} > 4 \text{ EeV}$                           | 50                         |
| number of stations $> 5$                           | 40                         |
| reduced $\chi^2$ of LDF fit $< 5$                  | 37                         |
| relative $E_{EM}$ uncertainty $< 0.2$              | 32                         |

#### 4. Measurement of the muon content

In the following, the AERA data recorded between 26 June 2013 (start of AERA phase II) and 1 Mai 2019 (last date for which we have bad periods) are analyzed. The same event selection as in Sec. 3 is applied. Furthermore, events that fall into thunderstorm periods [17] are excluded. This selection yields 32 high-quality hybrid events, the number of events after each cut is given in Tab. 1. The strongest cut is the minimum energy of 4 EeV due to the size of AERA.

The muon content in data is shown in Fig. 4 as a function of  $S_{\text{rad}}$ . The profile indicates an increasing number of muons for increasing values of  $S_{\text{rad}}$ , ie. with increasing energy. The measured muon content is compatible with the prediction of hadronic interaction models for iron nuclei. A thorough estimation of the systematic uncertainties will be done in a future publication. The expected mass composition can be derived from  $X_{\text{max}}$  measurement of the Auger FD. In the energy range of this analysis, the mean atomic mass number is expected to be between proton and nitrogen [19]. Hence, one can conclude that there is a deficit of muons in simulations. This was already found by other Auger analyses for primary energies above 4 EeV [20] as well as for primary energies between  $2 \cdot 10^{17}$  eV and  $2 \cdot 10^{18}$  eV [21].

#### 5. Conclusion

We showed a first estimate of the muon content of inclined air showers using hybrid measurements combining radio and particle detection. This serves as a proof of concept for future analyses with hybrid radio and particle events. We find a muon content in data that is compatible with the prediction of hadronic interaction models for iron-induced air showers even though the composition is expected to be between proton and nitrogen. This is the first time that it is demonstrated that hybrid detection of the radio emission and the particles can be used to investigate the already known muon puzzle.

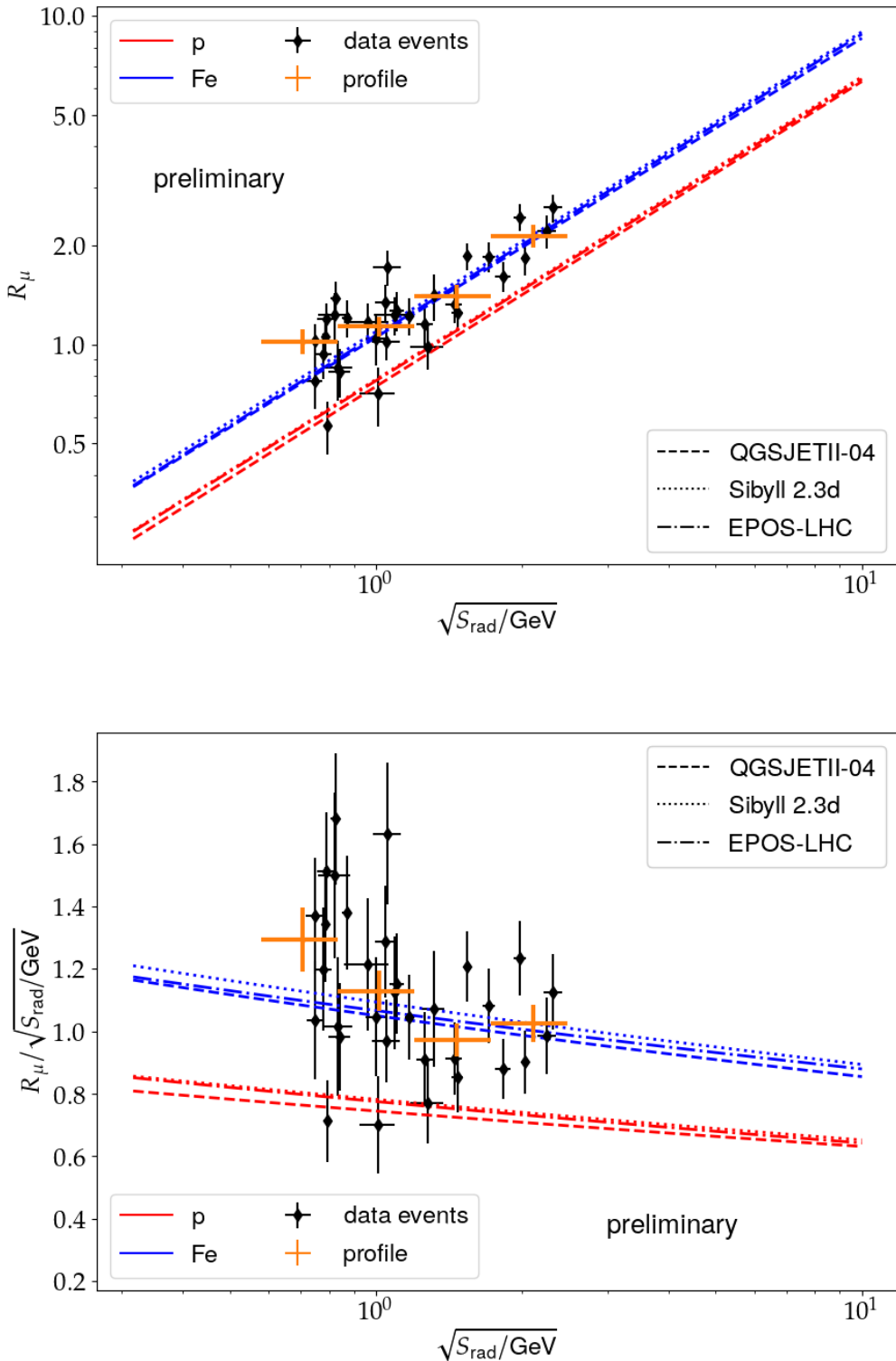


**Figure 4:** Muon content as a function of energy estimator (top) and normalized muon content (bottom) to remove the power-law scaling. In both figures, the model predictions are identical to Fig. 3. Measured data are shown in black, a profile of the data is given in orange.

Currently, the analysis is limited by the low statistics of 32 high-quality events which originate from the small area of AERA of  $17 \text{ km}^2$  and the high energy threshold of 4 EeV needed for the reconstruction with the 1500 m WCD array. The event statistics can be increased moderately by including 4 more years of data in a future publication. A reconstruction of inclined air shower with the 750 m WCD array is currently being developed which will allow reducing the energy threshold considerably and therefore collect more statistics at energies below 4 EeV. With the AugerPrime Radio Detector currently being deployed, this analysis can be extended to the highest energies to allow for in-depth tests of hadronic interaction models with large statistics [22].

## References

- [1] D. Soldin *et al.* PoS(ICRC2021)349
- [2] E.M. Holt *et al.* Eur. Phys. J. C **79** (2019) 371
- [3] A. Aab *et al.* [Pierre Auger coll.], JCAP **10** (2018) 26
- [4] M. Gottowik for the Pierre Auger Collaboration, PoS(ICRC2019)274
- [5] A. Aab *et al.* [Pierre Auger coll.], Nucl. Instrum. Meth. A **798** (2015) 172
- [6] E. M. Holt for the Pierre Auger Collaboration, PoS(ICRC2017)492
- [7] P. Abreu *et al.* [Pierre Auger coll.], JINST **7** (2012) 10011
- [8] A. Aab *et al.* [Pierre Auger coll.], JCAP **08** (2014) 19
- [9] F. Schlüter and T. Huege, JCAP **01** (2023) 008
- [10] C. Glaser *et al.* JCAP **9** (2016) 24
- [11] A. Aab *et al.* [Pierre Auger coll.], Phys. Rev. D **100** (2019) 82003
- [12] D. Heck *et al.* FZKA Tech. Umw. Wis. B 6019, (1998)
- [13] S. Ostapchenko, Phys. Rev. D **83** (2011) 14018
- [14] T. Pierog *et al.* Phys. Rev. C **92** (2015) 34906
- [15] F. Riehn *et al.* Phys. Rev. D **100** (2019) 103018
- [16] T. Huege *et al.* AIP Conf. Proc. **1535** (2013) 128
- [17] M. Gottowik. PhD thesis. (2021)  
<http://elpub.bib.uni-wuppertal.de/edocs/dokumente/fbc/physik/diss2021/gottowik>
- [18] J. Pawlowsky for the Pierre Auger Collaboration, PoS(ICRC2023)344
- [19] A. Yushkov for the Pierre Auger Collaboration, PoS(ICRC2019)482
- [20] A. Aab *et al.* [Pierre Auger coll.], Phys. Rev. Lett. **126** (2021) 152002
- [21] A. Aab *et al.* [Pierre Auger coll.], Eur. Phys. J. C **80** (2020) 751
- [22] T. Huege for the Pierre Auger Collaboration, EPJ Web Conf. **283** (2023) 6002

## The Pierre Auger Collaboration



PIERRE  
AUGER  
OBSERVATORY

- A. Abdul Halim<sup>13</sup>, P. Abreu<sup>72</sup>, M. Aglietta<sup>54,52</sup>, I. Allekotte<sup>1</sup>, K. Almeida Cheminant<sup>70</sup>, A. Almela<sup>7,12</sup>, R. Aloisio<sup>45,46</sup>, J. Alvarez-Muñiz<sup>79</sup>, J. Ammerman Yebra<sup>79</sup>, G.A. Anastasi<sup>54,52</sup>, L. Anchordoqui<sup>86</sup>, B. Andrada<sup>7</sup>, S. Andringa<sup>72</sup>, C. Aramo<sup>50</sup>, P.R. Araújo Ferreira<sup>42</sup>, E. Arnone<sup>63,52</sup>, J.C. Arteaga Velázquez<sup>67</sup>, H. Asorey<sup>7</sup>, P. Assis<sup>72</sup>, G. Avila<sup>11</sup>, E. Avocone<sup>57,46</sup>, A.M. Badescu<sup>75</sup>, A. Bakalova<sup>32</sup>, A. Balaceanu<sup>73</sup>, F. Barbato<sup>45,46</sup>, A. Bartz Mocellin<sup>85</sup>, J.A. Bellido<sup>13,69</sup>, C. Berat<sup>36</sup>, M.E. Bertaina<sup>63,52</sup>, G. Bhatta<sup>70</sup>, M. Bianciotto<sup>63,52</sup>, P.L. Biermann<sup>h</sup>, V. Binet<sup>5</sup>, K. Bismarck<sup>39,7</sup>, T. Bister<sup>80,81</sup>, J. Biteau<sup>37</sup>, J. Blazek<sup>32</sup>, C. Bleve<sup>36</sup>, J. Blümer<sup>41</sup>, M. Boháčová<sup>32</sup>, D. Boncioli<sup>57,46</sup>, C. Bonifazi<sup>8,26</sup>, L. Bonneau Arbeletche<sup>21</sup>, N. Borodai<sup>70</sup>, J. Brack<sup>j</sup>, P.G. Brichetto Orchera<sup>7</sup>, F.L. Brieche<sup>42</sup>, A. Bueno<sup>78</sup>, S. Buitink<sup>15</sup>, M. Buscemi<sup>47,61</sup>, M. Büsken<sup>39,7</sup>, A. Bwembya<sup>80,81</sup>, K.S. Caballero-Mora<sup>66</sup>, S. Cabana-Freire<sup>79</sup>, L. Caccianiga<sup>59,49</sup>, I. Caracas<sup>38</sup>, R. Caruso<sup>58,47</sup>, A. Castellina<sup>54,52</sup>, F. Catalani<sup>18</sup>, G. Cataldi<sup>48</sup>, L. Cazon<sup>79</sup>, M. Cerdá<sup>10</sup>, A. Cermenati<sup>45,46</sup>, J.A. Chinellato<sup>21</sup>, J. Chudoba<sup>32</sup>, L. Chytka<sup>33</sup>, R.W. Clay<sup>13</sup>, A.C. Cobos Cerutti<sup>6</sup>, R. Colalillo<sup>60,50</sup>, A. Coleman<sup>90</sup>, M.R. Coluccia<sup>48</sup>, R. Conceição<sup>72</sup>, A. Condorelli<sup>37</sup>, G. Consolati<sup>49,55</sup>, M. Conte<sup>56,48</sup>, F. Convenga<sup>41</sup>, D. Correia dos Santos<sup>28</sup>, P.J. Costa<sup>72</sup>, C.E. Covault<sup>84</sup>, M. Cristinziani<sup>44</sup>, C.S. Cruz Sanchez<sup>3</sup>, S. Dasso<sup>4,2</sup>, K. Daumiller<sup>41</sup>, B.R. Dawson<sup>13</sup>, R.M. de Almeida<sup>28</sup>, J. de Jesús<sup>7,41</sup>, S.J. de Jong<sup>80,81</sup>, J.R.T. de Mello Neto<sup>26,27</sup>, I. De Mitri<sup>45,46</sup>, J. de Oliveira<sup>17</sup>, D. de Oliveira Franco<sup>21</sup>, F. de Palma<sup>56,48</sup>, V. de Souza<sup>19</sup>, E. De Vito<sup>56,48</sup>, A. Del Popolo<sup>58,47</sup>, O. Deligny<sup>34</sup>, N. Denner<sup>32</sup>, L. Deval<sup>41,7</sup>, A. di Matteo<sup>52</sup>, M. Dobre<sup>73</sup>, C. Dobrigkeit<sup>21</sup>, J.C. D'Olivo<sup>68</sup>, L.M. Domingues Mendes<sup>72</sup>, J.C. dos Anjos, R.C. dos Anjos<sup>25</sup>, J. Ebr<sup>32</sup>, F. Ellwanger<sup>41</sup>, M. Emam<sup>80,81</sup>, R. Engel<sup>39,41</sup>, I. Epicoco<sup>56,48</sup>, M. Erdmann<sup>42</sup>, A. Etchegoyen<sup>7,12</sup>, C. Evoli<sup>45,46</sup>, H. Falcke<sup>80,82,81</sup>, J. Farmer<sup>89</sup>, G. Farrar<sup>88</sup>, A.C. Fauth<sup>21</sup>, N. Fazzini<sup>e</sup>, F. Feldbusch<sup>40</sup>, F. Fenu<sup>41,d</sup>, A. Fernandes<sup>72</sup>, B. Fick<sup>87</sup>, J.M. Figueira<sup>7</sup>, A. Filipčič<sup>77,76</sup>, T. Fitoussi<sup>41</sup>, B. Flaggs<sup>90</sup>, T. Fodran<sup>80</sup>, T. Fujii<sup>89,f</sup>, A. Fuster<sup>7,12</sup>, C. Galea<sup>80</sup>, C. Galelli<sup>59,49</sup>, B. García<sup>6</sup>, C. Gaudu<sup>38</sup>, H. Gemmeke<sup>40</sup>, F. Gesualdi<sup>7,41</sup>, A. Gherghel-Lascu<sup>73</sup>, P.L. Ghia<sup>34</sup>, U. Giaccari<sup>48</sup>, M. Giammarchi<sup>49</sup>, J. Glombitzka<sup>42,8</sup>, F. Gobbi<sup>10</sup>, F. Gollan<sup>7</sup>, G. Golup<sup>1</sup>, M. Gómez Berisso<sup>1</sup>, P.F. Gómez Vitale<sup>11</sup>, J.P. Gongora<sup>11</sup>, J.M. González<sup>1</sup>, N. González<sup>7</sup>, I. Goos<sup>1</sup>, D. Góra<sup>70</sup>, A. Gorgi<sup>54,52</sup>, M. Gottowik<sup>79</sup>, T.D. Grubb<sup>13</sup>, F. Guarino<sup>60,50</sup>, G.P. Guedes<sup>22</sup>, E. Guido<sup>44</sup>, S. Hahn<sup>39</sup>, P. Hamal<sup>32</sup>, M.R. Hampel<sup>7</sup>, P. Hansen<sup>3</sup>, D. Harari<sup>1</sup>, V.M. Harvey<sup>13</sup>, A. Haungs<sup>41</sup>, T. Hebbeker<sup>42</sup>, C. Hojvat<sup>e</sup>, J.R. Hörandel<sup>80,81</sup>, P. Horvath<sup>33</sup>, M. Hrabovský<sup>33</sup>, T. Huege<sup>41,15</sup>, A. Insolia<sup>58,47</sup>, P.G. Isar<sup>74</sup>, P. Janecek<sup>32</sup>, J.A. Johnsen<sup>85</sup>, J. Jurysek<sup>32</sup>, A. Kääpä<sup>38</sup>, K.H. Kampert<sup>38</sup>, B. Keilhauer<sup>41</sup>, A. Khakurdikar<sup>80</sup>, V.V. Kizakke Covilakam<sup>7,41</sup>, H.O. Klages<sup>41</sup>, M. Kleifges<sup>40</sup>, F. Knapp<sup>39</sup>, N. Kunka<sup>40</sup>, B.L. Lago<sup>16</sup>, N. Langner<sup>42</sup>, M.A. Leigui de Oliveira<sup>24</sup>, Y Lema-Capeans<sup>79</sup>, V. Lenok<sup>39</sup>, A. Letessier-Selvon<sup>35</sup>, I. Lhenry-Yvon<sup>34</sup>, D. Lo Presti<sup>58,47</sup>, L. Lopes<sup>72</sup>, L. Lu<sup>91</sup>, Q. Luce<sup>39</sup>, J.P. Lundquist<sup>76</sup>, A. Machado Payeras<sup>21</sup>, M. Majercakova<sup>32</sup>, D. Mandat<sup>32</sup>, B.C. Manning<sup>13</sup>, P. Mantsch<sup>e</sup>, S. Marafico<sup>34</sup>, F.M. Mariami<sup>59,49</sup>, A.G. Mariazzi<sup>3</sup>, I.C. Mariş<sup>14</sup>, G. Marsella<sup>61,47</sup>, D. Martello<sup>56,48</sup>, S. Martinelli<sup>41,7</sup>, O. Martínez Bravo<sup>64</sup>, M.A. Martins<sup>79</sup>, M. Mastrodicasa<sup>57,46</sup>, H.J. Mathes<sup>41</sup>, J. Matthews<sup>a</sup>, G. Matthiae<sup>62,51</sup>, E. Mayotte<sup>85,38</sup>, S. Mayotte<sup>85</sup>, P.O. Mazur<sup>e</sup>, G. Medina-Tanco<sup>68</sup>, J. Meinert<sup>38</sup>, D. Melo<sup>7</sup>, A. Menshikov<sup>40</sup>, C. Merx<sup>41</sup>, S. Michal<sup>33</sup>, M.I. Micheletti<sup>5</sup>, L. Miramonti<sup>59,49</sup>, S. Mollerach<sup>1</sup>, F. Montanet<sup>36</sup>, L. Morejon<sup>38</sup>, C. Morello<sup>54,52</sup>, A.L. Müller<sup>32</sup>, K. Mulrey<sup>80,81</sup>, R. Mussa<sup>52</sup>, M. Muzio<sup>88</sup>, W.M. Namasaka<sup>38</sup>, S. Negi<sup>32</sup>, L. Nellen<sup>68</sup>, K. Nguyen<sup>87</sup>, G. Nicora<sup>9</sup>, M. Niculescu-Oglizanu<sup>73</sup>, M. Niechciol<sup>44</sup>, D. Nitz<sup>87</sup>, D. Nosek<sup>31</sup>, V. Novotny<sup>31</sup>, L. Nožka<sup>33</sup>, A. Nucita<sup>56,48</sup>, L.A. Núñez<sup>30</sup>, C. Oliveira<sup>19</sup>, M. Palatka<sup>32</sup>, J. Pallotta<sup>9</sup>, S. Panja<sup>32</sup>, G. Parente<sup>79</sup>, T. Paulsen<sup>38</sup>, J. Pawlowsky<sup>38</sup>, M. Pech<sup>32</sup>, J. Pěkala<sup>70</sup>, R. Pelayo<sup>65</sup>, L.A.S. Pereira<sup>23</sup>, E.E. Pereira Martins<sup>39,7</sup>, J. Perez Armand<sup>20</sup>, C. Pérez Bertolli<sup>7,41</sup>, L. Perrone<sup>56,48</sup>, S. Petrera<sup>45,46</sup>, C. Petrucci<sup>57,46</sup>, T. Pierog<sup>41</sup>, M. Pimenta<sup>72</sup>, M. Platino<sup>7</sup>, B. Pont<sup>80</sup>, M. Pothast<sup>81,80</sup>, M. Pourmohammad Shahvar<sup>61,47</sup>, P. Privitera<sup>89</sup>, M. Prouza<sup>32</sup>, A. Puyleart<sup>87</sup>, S. Querchfeld<sup>38</sup>, J. Rautenberg<sup>38</sup>, D. Ravignani<sup>7</sup>, M. Reininghaus<sup>39</sup>, J. Ridky<sup>32</sup>, F. Riehn<sup>79</sup>, M. Risso<sup>44</sup>, V. Rizi<sup>57,46</sup>, W. Rodrigues de Carvalho<sup>80</sup>, E. Rodriguez<sup>7,41</sup>, J. Rodriguez Rojo<sup>11</sup>, M.J. Roncoroni<sup>7</sup>, S. Rossoni<sup>43</sup>, M. Roth<sup>41</sup>, E. Roulet<sup>1</sup>, A.C. Rovero<sup>4</sup>, P. Ruehl<sup>44</sup>, A. Saftoiu<sup>73</sup>, M. Saharan<sup>80</sup>, F. Salamida<sup>57,46</sup>, H. Salazar<sup>64</sup>, G. Salina<sup>51</sup>, J.D. Sanabria Gomez<sup>30</sup>, F. Sánchez<sup>7</sup>, E.M. Santos<sup>20</sup>, E. Santos<sup>32</sup>,

F. Sarazin<sup>85</sup>, R. Sarmento<sup>72</sup>, R. Sato<sup>11</sup>, P. Savina<sup>91</sup>, C.M. Schäfer<sup>41</sup>, V. Scherini<sup>56,48</sup>, H. Schieler<sup>41</sup>, M. Schimassek<sup>34</sup>, M. Schimp<sup>38</sup>, F. Schlüter<sup>41</sup>, D. Schmidt<sup>39</sup>, O. Scholten<sup>15,i</sup>, H. Schoorlemmer<sup>80,81</sup>, P. Schovánek<sup>32</sup>, F.G. Schröder<sup>90,41</sup>, J. Schulte<sup>42</sup>, T. Schulz<sup>41</sup>, S.J. Sciutto<sup>3</sup>, M. Scornavacche<sup>7,41</sup>, A. Segreto<sup>53,47</sup>, S. Sehgal<sup>38</sup>, S.U. Shivashankara<sup>76</sup>, G. Sigl<sup>43</sup>, G. Silli<sup>7</sup>, O. Sima<sup>73,b</sup>, F. Simon<sup>40</sup>, R. Smau<sup>73</sup>, R. Šmídá<sup>89</sup>, P. Sommers<sup>k</sup>, J.F. Soriano<sup>86</sup>, R. Squartini<sup>10</sup>, M. Stadelmaier<sup>32</sup>, D. Stanca<sup>73</sup>, S. Stanič<sup>76</sup>, J. Stasielak<sup>70</sup>, P. Stassi<sup>36</sup>, S. Strähnz<sup>39</sup>, M. Straub<sup>42</sup>, M. Suárez-Durán<sup>14</sup>, T. Suomijärvi<sup>37</sup>, A.D. Supanitsky<sup>7</sup>, Z. Svozilikova<sup>32</sup>, Z. Szadkowski<sup>71</sup>, A. Tapia<sup>29</sup>, C. Taricco<sup>63,52</sup>, C. Timmermans<sup>81,80</sup>, O. Tkachenko<sup>41</sup>, P. Tobiska<sup>32</sup>, C.J. Todero Peixoto<sup>18</sup>, B. Tomé<sup>72</sup>, Z. Torrès<sup>36</sup>, A. Travaini<sup>10</sup>, P. Travnicek<sup>32</sup>, C. Trimarelli<sup>57,46</sup>, M. Tueros<sup>3</sup>, M. Unger<sup>41</sup>, L. Vaclavek<sup>33</sup>, M. Vacula<sup>33</sup>, J.F. Valdés Galicia<sup>68</sup>, L. Valore<sup>60,50</sup>, E. Varela<sup>64</sup>, A. Vásquez-Ramírez<sup>30</sup>, D. Veberič<sup>41</sup>, C. Ventura<sup>27</sup>, I.D. Vergara Quispe<sup>3</sup>, V. Verzi<sup>51</sup>, J. Vicha<sup>32</sup>, J. Vink<sup>83</sup>, J. Vlastimil<sup>32</sup>, S. Vorobiov<sup>76</sup>, C. Watanabe<sup>26</sup>, A.A. Watson<sup>c</sup>, A. Weindl<sup>41</sup>, L. Wiencke<sup>85</sup>, H. Wilczyński<sup>70</sup>, D. Wittkowski<sup>38</sup>, B. Wundheiler<sup>7</sup>, B. Yue<sup>38</sup>, A. Yushkov<sup>32</sup>, O. Zapparrata<sup>14</sup>, E. Zas<sup>79</sup>, D. Zavrtanik<sup>76,77</sup>, M. Zavrtanik<sup>77,76</sup>

<sup>1</sup> Centro Atómico Bariloche and Instituto Balseiro (CNEA-UNCuyo-CONICET), San Carlos de Bariloche, Argentina<sup>2</sup> Departamento de Física and Departamento de Ciencias de la Atmósfera y los Océanos, FCEyN, Universidad de Buenos Aires and CONICET, Buenos Aires, Argentina<sup>3</sup> IFLP, Universidad Nacional de La Plata and CONICET, La Plata, Argentina<sup>4</sup> Instituto de Astronomía y Física del Espacio (IAFE, CONICET-UBA), Buenos Aires, Argentina<sup>5</sup> Instituto de Física de Rosario (IFIR) – CONICET/U.N.R. and Facultad de Ciencias Bioquímicas y Farmacéuticas U.N.R., Rosario, Argentina<sup>6</sup> Instituto de Tecnologías en Detección y Astropartículas (CNEA, CONICET, UNSAM), and Universidad Tecnológica Nacional – Facultad Regional Mendoza (CONICET/CNEA), Mendoza, Argentina<sup>7</sup> Instituto de Tecnologías en Detección y Astropartículas (CNEA, CONICET, UNSAM), Buenos Aires, Argentina<sup>8</sup> International Center of Advanced Studies and Instituto de Ciencias Físicas, ECyT-UNSAM and CONICET, Campus Miguelete – San Martín, Buenos Aires, Argentina<sup>9</sup> Laboratorio Atmósfera – Departamento de Investigaciones en Láseres y sus Aplicaciones – UNIDEF (CITEDEF-CONICET), Argentina<sup>10</sup> Observatorio Pierre Auger, Malargüe, Argentina<sup>11</sup> Observatorio Pierre Auger and Comisión Nacional de Energía Atómica, Malargüe, Argentina<sup>12</sup> Universidad Tecnológica Nacional – Facultad Regional Buenos Aires, Buenos Aires, Argentina<sup>13</sup> University of Adelaide, Adelaide, S.A., Australia<sup>14</sup> Université Libre de Bruxelles (ULB), Brussels, Belgium<sup>15</sup> Vrije Universiteit Brussels, Brussels, Belgium<sup>16</sup> Centro Federal de Educação Tecnológica Celso Suckow da Fonseca, Petropolis, Brazil<sup>17</sup> Instituto Federal de Educação, Ciência e Tecnologia do Rio de Janeiro (IFRJ), Brazil<sup>18</sup> Universidade de São Paulo, Escola de Engenharia de Lorena, Lorena, SP, Brazil<sup>19</sup> Universidade de São Paulo, Instituto de Física de São Carlos, São Carlos, SP, Brazil<sup>20</sup> Universidade de São Paulo, Instituto de Física, São Paulo, SP, Brazil<sup>21</sup> Universidade Estadual de Campinas, IFGW, Campinas, SP, Brazil<sup>22</sup> Universidade Estadual de Feira de Santana, Feira de Santana, Brazil<sup>23</sup> Universidade Federal de Campina Grande, Centro de Ciencias e Tecnologia, Campina Grande, Brazil<sup>24</sup> Universidade Federal do ABC, Santo André, SP, Brazil<sup>25</sup> Universidade Federal do Paraná, Setor Palotina, Palotina, Brazil<sup>26</sup> Universidade Federal do Rio de Janeiro, Instituto de Física, Rio de Janeiro, RJ, Brazil<sup>27</sup> Universidade Federal do Rio de Janeiro (UFRJ), Observatório do Valongo, Rio de Janeiro, RJ, Brazil<sup>28</sup> Universidade Federal Fluminense, EEIMVR, Volta Redonda, RJ, Brazil<sup>29</sup> Universidad de Medellín, Medellín, Colombia<sup>30</sup> Universidad Industrial de Santander, Bucaramanga, Colombia

- <sup>31</sup> Charles University, Faculty of Mathematics and Physics, Institute of Particle and Nuclear Physics, Prague, Czech Republic
- <sup>32</sup> Institute of Physics of the Czech Academy of Sciences, Prague, Czech Republic
- <sup>33</sup> Palacky University, Olomouc, Czech Republic
- <sup>34</sup> CNRS/IN2P3, IJCLab, Université Paris-Saclay, Orsay, France
- <sup>35</sup> Laboratoire de Physique Nucléaire et de Hautes Energies (LPNHE), Sorbonne Université, Université de Paris, CNRS-IN2P3, Paris, France
- <sup>36</sup> Univ. Grenoble Alpes, CNRS, Grenoble Institute of Engineering Univ. Grenoble Alpes, LPSC-IN2P3, 38000 Grenoble, France
- <sup>37</sup> Université Paris-Saclay, CNRS/IN2P3, IJCLab, Orsay, France
- <sup>38</sup> Bergische Universität Wuppertal, Department of Physics, Wuppertal, Germany
- <sup>39</sup> Karlsruhe Institute of Technology (KIT), Institute for Experimental Particle Physics, Karlsruhe, Germany
- <sup>40</sup> Karlsruhe Institute of Technology (KIT), Institut für Prozessdatenverarbeitung und Elektronik, Karlsruhe, Germany
- <sup>41</sup> Karlsruhe Institute of Technology (KIT), Institute for Astroparticle Physics, Karlsruhe, Germany
- <sup>42</sup> RWTH Aachen University, III. Physikalisches Institut A, Aachen, Germany
- <sup>43</sup> Universität Hamburg, II. Institut für Theoretische Physik, Hamburg, Germany
- <sup>44</sup> Universität Siegen, Department Physik – Experimentelle Teilchenphysik, Siegen, Germany
- <sup>45</sup> Gran Sasso Science Institute, L'Aquila, Italy
- <sup>46</sup> INFN Laboratori Nazionali del Gran Sasso, Assergi (L'Aquila), Italy
- <sup>47</sup> INFN, Sezione di Catania, Catania, Italy
- <sup>48</sup> INFN, Sezione di Lecce, Lecce, Italy
- <sup>49</sup> INFN, Sezione di Milano, Milano, Italy
- <sup>50</sup> INFN, Sezione di Napoli, Napoli, Italy
- <sup>51</sup> INFN, Sezione di Roma “Tor Vergata”, Roma, Italy
- <sup>52</sup> INFN, Sezione di Torino, Torino, Italy
- <sup>53</sup> Istituto di Astrofisica Spaziale e Fisica Cosmica di Palermo (INAF), Palermo, Italy
- <sup>54</sup> Osservatorio Astrofisico di Torino (INAF), Torino, Italy
- <sup>55</sup> Politecnico di Milano, Dipartimento di Scienze e Tecnologie Aeroespaziali , Milano, Italy
- <sup>56</sup> Università del Salento, Dipartimento di Matematica e Fisica “E. De Giorgi”, Lecce, Italy
- <sup>57</sup> Università dell'Aquila, Dipartimento di Scienze Fisiche e Chimiche, L'Aquila, Italy
- <sup>58</sup> Università di Catania, Dipartimento di Fisica e Astronomia “Ettore Majorana“, Catania, Italy
- <sup>59</sup> Università di Milano, Dipartimento di Fisica, Milano, Italy
- <sup>60</sup> Università di Napoli “Federico II”, Dipartimento di Fisica “Ettore Pancini”, Napoli, Italy
- <sup>61</sup> Università di Palermo, Dipartimento di Fisica e Chimica ”E. Segrè”, Palermo, Italy
- <sup>62</sup> Università di Roma “Tor Vergata”, Dipartimento di Fisica, Roma, Italy
- <sup>63</sup> Università Torino, Dipartimento di Fisica, Torino, Italy
- <sup>64</sup> Benemérita Universidad Autónoma de Puebla, Puebla, México
- <sup>65</sup> Unidad Profesional Interdisciplinaria en Ingeniería y Tecnologías Avanzadas del Instituto Politécnico Nacional (UPIITA-IPN), México, D.F., México
- <sup>66</sup> Universidad Autónoma de Chiapas, Tuxtla Gutiérrez, Chiapas, México
- <sup>67</sup> Universidad Michoacana de San Nicolás de Hidalgo, Morelia, Michoacán, México
- <sup>68</sup> Universidad Nacional Autónoma de México, México, D.F., México
- <sup>69</sup> Universidad Nacional de San Agustín de Arequipa, Facultad de Ciencias Naturales y Formales, Arequipa, Peru
- <sup>70</sup> Institute of Nuclear Physics PAN, Krakow, Poland
- <sup>71</sup> University of Łódź, Faculty of High-Energy Astrophysics, Łódź, Poland
- <sup>72</sup> Laboratório de Instrumentação e Física Experimental de Partículas – LIP and Instituto Superior Técnico – IST, Universidade de Lisboa – UL, Lisboa, Portugal
- <sup>73</sup> “Horia Hulubei” National Institute for Physics and Nuclear Engineering, Bucharest-Magurele, Romania
- <sup>74</sup> Institute of Space Science, Bucharest-Magurele, Romania
- <sup>75</sup> University Politehnica of Bucharest, Bucharest, Romania
- <sup>76</sup> Center for Astrophysics and Cosmology (CAC), University of Nova Gorica, Nova Gorica, Slovenia
- <sup>77</sup> Experimental Particle Physics Department, J. Stefan Institute, Ljubljana, Slovenia

- <sup>78</sup> Universidad de Granada and C.A.F.P.E., Granada, Spain  
<sup>79</sup> Instituto Galego de Física de Altas Enerxías (IGFAE), Universidade de Santiago de Compostela, Santiago de Compostela, Spain  
<sup>80</sup> IMAPP, Radboud University Nijmegen, Nijmegen, The Netherlands  
<sup>81</sup> Nationaal Instituut voor Kernfysica en Hoge Energie Fysica (NIKHEF), Science Park, Amsterdam, The Netherlands  
<sup>82</sup> Stichting Astronomisch Onderzoek in Nederland (ASTRON), Dwingeloo, The Netherlands  
<sup>83</sup> Universiteit van Amsterdam, Faculty of Science, Amsterdam, The Netherlands  
<sup>84</sup> Case Western Reserve University, Cleveland, OH, USA  
<sup>85</sup> Colorado School of Mines, Golden, CO, USA  
<sup>86</sup> Department of Physics and Astronomy, Lehman College, City University of New York, Bronx, NY, USA  
<sup>87</sup> Michigan Technological University, Houghton, MI, USA  
<sup>88</sup> New York University, New York, NY, USA  
<sup>89</sup> University of Chicago, Enrico Fermi Institute, Chicago, IL, USA  
<sup>90</sup> University of Delaware, Department of Physics and Astronomy, Bartol Research Institute, Newark, DE, USA  
<sup>91</sup> University of Wisconsin-Madison, Department of Physics and WIPAC, Madison, WI, USA

---

<sup>a</sup> Louisiana State University, Baton Rouge, LA, USA

<sup>b</sup> also at University of Bucharest, Physics Department, Bucharest, Romania

<sup>c</sup> School of Physics and Astronomy, University of Leeds, Leeds, United Kingdom

<sup>d</sup> now at Agenzia Spaziale Italiana (ASI). Via del Politecnico 00133, Roma, Italy

<sup>e</sup> Fermi National Accelerator Laboratory, Fermilab, Batavia, IL, USA

<sup>f</sup> now at Graduate School of Science, Osaka Metropolitan University, Osaka, Japan

<sup>g</sup> now at ECAP, Erlangen, Germany

<sup>h</sup> Max-Planck-Institut für Radioastronomie, Bonn, Germany

<sup>i</sup> also at Kapteyn Institute, University of Groningen, Groningen, The Netherlands

<sup>j</sup> Colorado State University, Fort Collins, CO, USA

<sup>k</sup> Pennsylvania State University, University Park, PA, USA

## Acknowledgments

The successful installation, commissioning, and operation of the Pierre Auger Observatory would not have been possible without the strong commitment and effort from the technical and administrative staff in Malargüe. We are very grateful to the following agencies and organizations for financial support:

Argentina – Comisión Nacional de Energía Atómica; Agencia Nacional de Promoción Científica y Tecnológica (ANPCyT); Consejo Nacional de Investigaciones Científicas y Técnicas (CONICET); Gobierno de la Provincia de Mendoza; Municipalidad de Malargüe; NDM Holdings and Valle Las Leñas; in gratitude for their continuing cooperation over land access; Australia – the Australian Research Council; Belgium – Fonds de la Recherche Scientifique (FNRS); Research Foundation Flanders (FWO); Brazil – Conselho Nacional de Desenvolvimento Científico e Tecnológico (CNPq); Financiadora de Estudos e Projetos (FINEP); Fundação de Amparo à Pesquisa do Estado de Rio de Janeiro (FAPERJ); São Paulo Research Foundation (FAPESP) Grants No. 2019/10151-2, No. 2010/07359-6 and No. 1999/05404-3; Ministério da Ciência, Tecnologia, Inovações e Comunicações (MCTIC); Czech Republic – Grant No. MSMT CR LTT18004, LM2015038, LM2018102, CZ.02.1.01/0.0/0.0/16\_013/0001402, CZ.02.1.01/0.0/0.0/18\_046/0016010 and CZ.02.1.01/0.0/0.0/17\_049/0008422; France – Centre de Calcul IN2P3/CNRS; Centre National de la Recherche Scientifique (CNRS); Conseil Régional Ile-de-France; Département Physique Nucléaire et Corpusculaire (DNC-IN2P3/CNRS); Département Sciences de l'Univers (SDU-INSU/CNRS); Institut Lagrange de Paris (ILP) Grant No. LABEX ANR-10-LABX-63 within the Investissements d'Avenir Programme Grant No. ANR-11-IDEX-0004-02; Germany – Bundesministerium für Bildung und Forschung (BMBF); Deutsche Forschungsgemeinschaft (DFG); Finanzministerium Baden-Württemberg; Helmholtz Alliance for Astroparticle Physics (HAP); Helmholtz-Gemeinschaft Deutscher Forschungszentren (HGF); Ministerium für Kultur und Wissenschaft des Landes Nordrhein-Westfalen; Ministerium für Wissenschaft, Forschung und Kunst des Landes Baden-Württemberg; Italy – Istituto Nazionale di Fisica Nucleare (INFN); Istituto Nazionale di Astrofisica (INAF); Ministero dell'Università e della Ricerca (MUR); CETEMPS Center of Excellence; Ministero degli Affari Esteri (MAE), ICSC Centro Nazionale di Ricerca in High Performance Computing, Big Data

and Quantum Computing, funded by European Union NextGenerationEU, reference code CN\_00000013; México – Consejo Nacional de Ciencia y Tecnología (CONACYT) No. 167733; Universidad Nacional Autónoma de México (UNAM); PAPIIT DGAPA-UNAM; The Netherlands – Ministry of Education, Culture and Science; Netherlands Organisation for Scientific Research (NWO); Dutch national e-infrastructure with the support of SURF Cooperative; Poland – Ministry of Education and Science, grants No. DIR/WK/2018/11 and 2022/WK/12; National Science Centre, grants No. 2016/22/M/ST9/00198, 2016/23/B/ST9/01635, 2020/39/B/ST9/01398, and 2022/45/B/ST9/02163; Portugal – Portuguese national funds and FEDER funds within Programa Operacional Factores de Competitividade through Fundação para a Ciência e a Tecnologia (COMPETE); Romania – Ministry of Research, Innovation and Digitization, CNCS-UEFISCDI, contract no. 30N/2023 under Romanian National Core Program LAPLAS VII, grant no. PN 23/21/01/02 and project number PN-III-P1-1.1-TE-2021-0924/TE57/2022, within PNCDI III; Slovenia – Slovenian Research Agency, grants P1-0031, P1-0385, I0-0033, N1-0111; Spain – Ministerio de Economía, Industria y Competitividad (FPA2017-85114-P and PID2019-104676GB-C32), Xunta de Galicia (ED431C 2017/07), Junta de Andalucía (SOMM17/6104/UGR, P18-FR-4314) Feder Funds, RENATA Red Nacional Temática de Astropartículas (FPA2015-68783-REDT) and María de Maeztu Unit of Excellence (MDM-2016-0692); USA – Department of Energy, Contracts No. DE-AC02-07CH11359, No. DE-FR02-04ER41300, No. DE-FG02-99ER41107 and No. DE-SC0011689; National Science Foundation, Grant No. 0450696; The Grainger Foundation; Marie Curie-IRSES/EPLANET; European Particle Physics Latin American Network; and UNESCO.